GRIFFITH UNIVERSITY

Time evolution of graphene growth on SiC as a function of annealing temperature

Author

Zarotti, F., Gupta, B., Iacopi, Francesca, Sgarlata, A., Tomellini, M., Motta, Nunzio

Published

2016

Journal Title

Carbon

DOI

10.1016/j.carbon.2015.11.026

Rights statement

© 2016 Elsevier. Licensed under the Creative Commons Attribution-NonCommercial-NoDerivatives 4.0 International Licence (http://creativecommons.org/licenses/by-nc-nd/4.0/) which permits unrestricted, non-commercial use, distribution and reproduction in any medium, providing that the work is properly cited.

Downloaded from

http://hdl.handle.net/10072/99853

Griffith Research Online

https://research-repository.griffith.edu.au

Time evolution of graphene growth on SiC as a function of annealing temperature

F.Zarotti[1,2], B.Gupta[1], F.Iacopi[3], A.Sgarlata[2], M.Tomellini[4], N.Motta*[1]

[1] School of Chemistry Physics and Mechanical Engineering and Institute for Future Environments, Queensland University of Technology, 2 George Street, Brisbane 4001, QLD, Australia

[2]Dipartimento di Fisica, Università di Roma "Tor Vergata", via della Ricerca Scientifica 1, 00133 Roma.

[3] Queensland Micro and Nanotechnology Centre, Griffith University, Nathan Campus 4111, QLD Australia

[4]Dipartimento di Scienze e Tecnologie Chimiche, Università di Roma "Tor Vergata", via della Ricerca Scientifica 1, 00133 Roma.

Abstract

We followed by X-ray Photoelectron Spectroscopy (XPS) the time evolution of graphene layers obtained by annealing 3C SiC(111)/Si(111) crystals at different temperatures. The intensity of the carbon signal provides a quantification of the graphene thickness as a function of the annealing time, which follows a power law with exponent 0.5. We show that a kinetic model, based on a bottom-up growth mechanism, provides a full explanation to the evolution of the graphene thickness as a function of time, allowing to calculate the effective activation energy of the process and the energy barriers, in excellent agreement with previous theoretical results. Our study provides a complete and exhaustive picture of Si diffusion into the SiC matrix, establishing the conditions for a perfect control of the graphene growth by Si sublimation.

1. Introduction

After more than one decade from its discovery, Graphene is still attracting the interest of researchers because of its unique structural and electronic properties, which are expected to lead to new

applications in area as diverse as electronics [1], sensing [2], material reinforcement [3] and energy storage [4].

One of the main challenges in electronic applications is the quality of the graphene layers, which is still far from the level required to obtain an industrial scale production of reliable nanoscale devices, and it is ultimately related to the growth method. Understanding the kinetics of the graphene growth is an outstanding problem in physics, whose solution is the key to achieve full control on the graphene quality.

In the last few years several authors demonstrated the possibility of growing perfectly controlled layers of graphene on SiC(0001) by using thermal annealing in a furnace under Ar atmosphere [5], in a pressurized vessel [6] or in Ultra High Vacuum (UHV) under Si flux and N_2 partial pressure [7]. All these studies agree on the fact that Si sublimates too quickly in UHV. Thermal annealing of SiC in UHV, at temperatures where Si diffuses out from the surface, occurs in a non-equilibrium condition. To bring the system as close as possible to the equilibrium several strategies have been employed to limit the Si sublimation, obtaining large, continuous domains of high quality graphene films on SiC [8]. A number of studies have been devoted to the graphitization and formation of first layer [9-23], which occurs passing through several reconstructions. In particular, on the Si face it goes through the (3×3), $(\sqrt{3} \times \sqrt{3})R30^{\circ}$, $(6\sqrt{3} \times 6\sqrt{3})R30^{\circ}$ (interface layer between SiC and graphene made of C atoms) and finally (1×1) graphene.
Sun et al [24] analysed with the help of first principles calculations the diffusion of Si atoms through heptagon-pentagon defects of the $(6\sqrt{3} \times 6\sqrt{3})R30^{\circ}$ (defined $6\sqrt{3}$ in the following), demonstrating that after the formation of this structure, entirely made by C atoms, Si is no more exposed for an easy desorption. So the Si out diffusion becomes the rate-limiting step. They suggest two alternative pathways for the diffusion: vertically through the $6\sqrt{3}$ defects and laterally via a step edge. Huang et al and Hannon et al [25, 26] suggested a bottom up growth mode epitaxial graphene on SiC in UHV where upon annealing at high temperature the interface layer $6\sqrt{3}$ develops first, then turns into graphene, and then another interface layer is created underneath.
Tanaka et al [27] and Drabińska at al [28] reported a power law dependence of the number of graphene layers as a function of time, but they did not provide a full theory of the phenomenon.

As a matter of fact, a detailed theory of the epitaxial graphene formation by SiC thermal decomposition beyond the first layer is missing, and therefore it would be essential to develop a physical model to gain insight and achieve a perfect control on the phenomenon.

In the following we fill this gap by presenting a full model for the growth mechanism of multilayer epitaxial graphene by high temperature annealing of SiC. By analyzing the intensity of the XPS C 1s peak as a function of time and of the annealing temperature, we show that a kinetic model gives account of the time evolution of the graphene growth, confirming a layer-by-layer mode due to the out-diffusion of Si in SiC, and allowing to calculate the effective activation energy of the process.

2. Experimental

As received samples (250 nm thick 3C-SiC(111) layer on Si(111), grown by alternating supply epitaxy[29]) were cut to size (1.5×12) mm^2 and prepared as described elsewhere[30]. The samples were then introduced into our UHV system (base pressure in 10^{-11} mbar range), degassed at 600°C for a few hours in UHV and annealed at 950 °C for 10 minutes ($p_{max}=3 \cdot 10^{-10}$ mbar) in order to remove the native oxide. Four different samples were used, each undergoing the same pre-treatment but with a different final 30 minutes annealing step at T=1175, 1225, 1275 and 1325 ˚C, respectively. The 30 minutes timing is divided as follows: in the first 10 minutes the substrates were annealed in 1 minutes steps, each one followed by the acquisition of C and Si XPS spectra; in the following 10 minutes, the same procedure is applied every 2 minutes; and for the final 10 minutes every 5 minutes.

3. Results

Original C 1s spectra have been fitted using three different components: one referred to SiC (283 eV), one to graphene (G) (≈284.4 eV) and the other one to interface layer (I) (≈285.4 eV). An example of the adopted fitting procedure is displayed in Figure 1a for a sample annealed at 1175 ˚C for 30 minutes. The relative intensities of such components change during the annealing, showing an evolution in the surface composition as a function of the annealing time. In Figure 1b we report the evolution of the C 1s peaks as a function of time for T= 1225 ˚C, showing an evident change in the relative intensity of the SiC and G components. As expected the graphene component (G) is increasing while the SiC is decreasing.

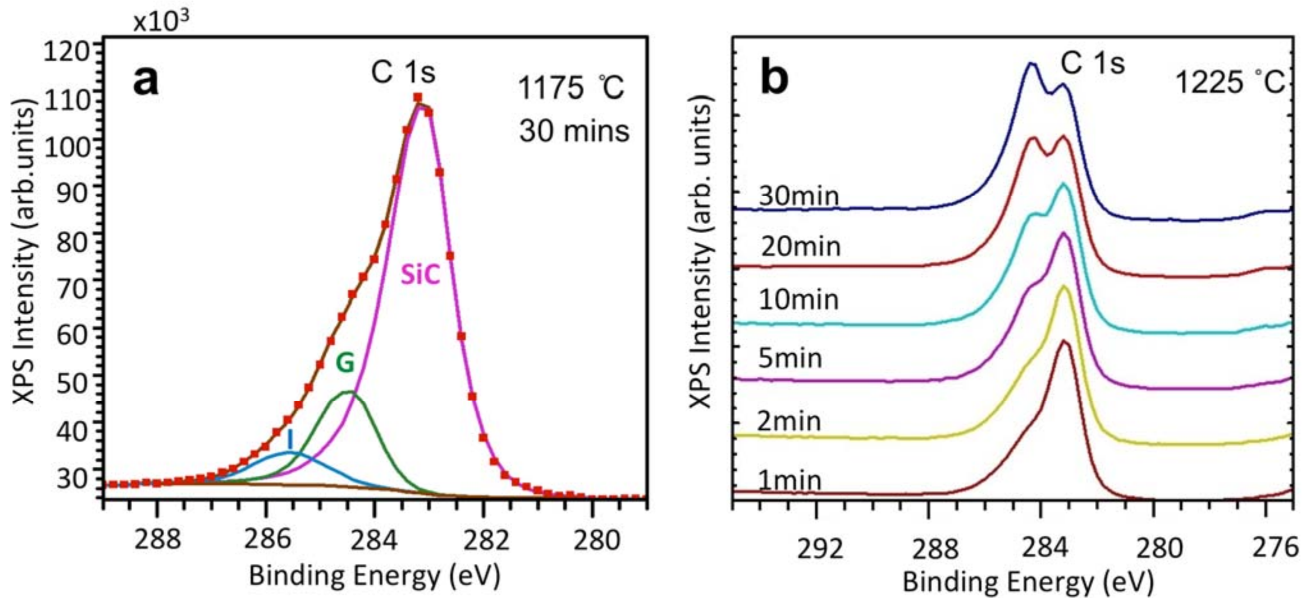

Figure 1: a) Fitting of XPS C1s peak with three different components identified as I (interface layer), G (graphene) and SiC. The spectrum refers to the growth of graphene for 30 minutes at 1175°C. (b) Time evolution of C1s spectra for graphene growth at 1225°C.

In order to quantify these variations we have defined the SiC peak as "substrate" component (I_{sub}), and the sum of G and I peaks as "overlayer" component (I_{ov}). An uncertainty of $\pm 5\%$ has been estimated for the XPS data.

Amongst different growth models (Volmer-Weber, Stranski-Krastanov, Frank Van Der Merwe), and considering a bottom-up mechanism for the development of the graphene layers, where Si atoms leave the buffer layer and C atoms rearrange in a new 2D network [5, 11, 31, 32], the best approach to explain our experimental data is to assume a *layer-by-layer* (Volmer-Weber) growth. It has been suggested that Si atoms can leave the buffer layer through holes of the top graphene layer or through a step edge [24], as depicted in a simplified way in Figure 2. In an early stage of formation, especially at lower temperatures, due to holes still present during the formation of the top layer, the first mechanism is the most probable*.

* We will not consider here the effect due diffusion through the step edge, which should become important at a later stage of the growth.

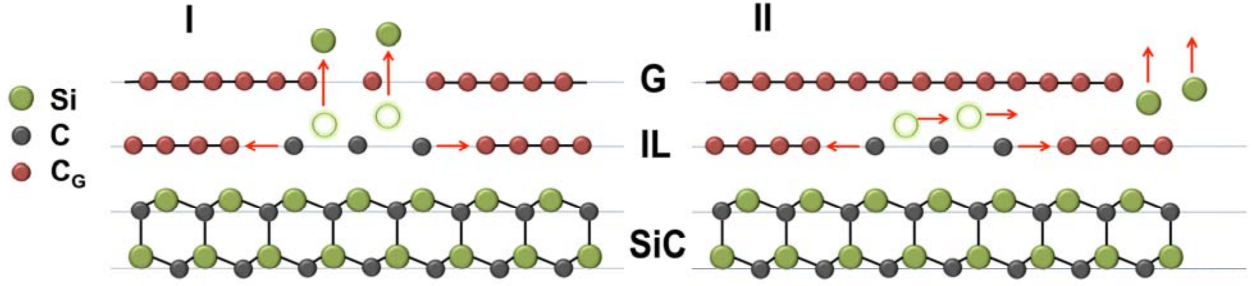

Figure 2:Simplified schematic representation of the epitaxial growth of graphene on SiC, according to two possible bottom-up mechanism [24]: I) If the top layer (G=graphene) is incomplete or defective Si atoms detach from the interface layer and diffuse through holes in the surface, leaving behind an excess of C atoms in the interface layer (IL), which is transformed in graphene when all Si is sublimated. II) When the top layer is completed Si atoms need to travel to a step edge in order to diffuse out of the surface.

In this assumption, XPS intensity signals for overlayer and substrate have been expressed as a function of *t*, such as:

$$\begin{cases} I_{ov}(t) = I_{ov}^{\infty}\left[1 - e^{-n(t)}\right] \\ I_{sub}(t) = I_{sub}^{0} e^{-n(t)} \end{cases} \quad (1)$$

where we define the adimensional function $n(t) = h(t)/\lambda$, as the ratio between $h(t)$, the mean overlayer thickness that form on substrate at the time *t*, and λ, the effective escape depth of electrons in the material. We note that the escape depth calculated from the TPP-2M[33] formula for graphene is λ=28 Å [34]; I_{ov}^{∞} is the (unknown) asymptotic value for the overlayer intensity; I_{sub}^{0} is the (known) value for the substrate intensity at $t = 0$. For the sake of simplicity, normalized expressions have been used:

$$\tilde{I}_{ov}(t) = \frac{I_{ov}^{\infty}}{\tilde{I}_{ov}^{0}}\left[1 - e^{-n(t)}\right] \quad (2)$$

$$\tilde{I}_{sub}(t) = \frac{I_{sub}^{0}}{I_{SiC}^{max}} e^{-n(t)} \quad (3)$$

where I_{sub}^{0} is a constant value equal to $2 \cdot 10^{5}$ and I_{SiC}^{max}, which is temperature dependent, is the maximum value of the experimental SiC component, such that $\frac{I_{sub}^{0}}{I_{SiC}^{max}} \approx 1$, as by definition the maximum intensity of the SiC component I_{SiC}^{max} coincides with the initial value of the substrate intensity I_{sub}^{0}. From equations (2) and (3) the following relation can be obtained:

$$\tilde{I}_{ov}(t) \approx m\left[1 - \tilde{I}_{sub}(t)\right] \quad (4)$$

Plotting the overlayer measured intensity versus the substrate intensity (see inset of Figure 3), it is possible to evaluate the slope, m, of Eqn (4), determining the unknown asymptotic value I_{ov}^{∞} for each temperature. By using the above values as parameters of Eqn. 2, a fitting of the overlayer data was obtained, considering a power growth law for the overlayer thickness in the form $n(t) = h(t)/\lambda = \beta t^{\gamma}$, being λ and β constants. The initial analysis has been carried out with two fitting parameters: β and γ. We found that $\gamma = 1/2$ is the common parameter providing the best fit at all temperatures. This defines the growth exponent, and confirms the hypothesis of a layer-by-layer growth mode. A new fitting, performed by using the formula:

$$n(t) = \beta\sqrt{t} \tag{5}$$

provides the value of the pre-factor β at each temperature. β has dimensions of $s^{-1/2}$ and $1/\beta^2$ can be considered as the characteristic time of the growth process. The results of the fits are displayed in Figure 3a. Values for β and $1/\beta^2$ are given in Table 1, at the four temperatures, along with the thickness of graphene layer $h(t_{max})$ calculated for each temperature at t=1800 s by using $h(t) = \lambda \cdot n(t)$.

T (˚C)	1175	1225	1275	1325
$\beta(s^{-1/2})$	3.8 10^{-3}	4.7 10^{-3}	14 10^{-3}	21 10^{-3}
$1/\beta^2$ (s)	69 10^{3}	46 10^{3}	5.3 10^{3}	2.3 10^{3}
$h(t_{max})$(Å)	4.5	5.6	16	21

Table 1. Values of β used in the fitting of $\tilde{I}_{ov}(t)$ by using Eqn. (2), along with the calculated $1/\beta^2$ and the thickness of graphene layer obtained at t=1800 s [34].

In order to prove the consistency of data analysis, once obtained the β values from the fitting of the overlayer, the substrate function $\tilde{I}_{sub}(t) = \frac{I_{sub}^{0}}{I_{SiC}^{max}} e^{-\beta\sqrt{t}}$ was calculated. The resulting functions have been reported at each T in Figure 3b, together with the XPS data of the substrate component $\tilde{I}_{sub}$. The general good agreement between the present analysis and the experimental data ensures the reliability of the self-consistent procedure adopted. The small deviation of the fitting from the data at 1325 ˚C suggests that at this temperature some other mechanism becomes predominant in the graphene formation. We will analyze this mechanism in the discussion section.

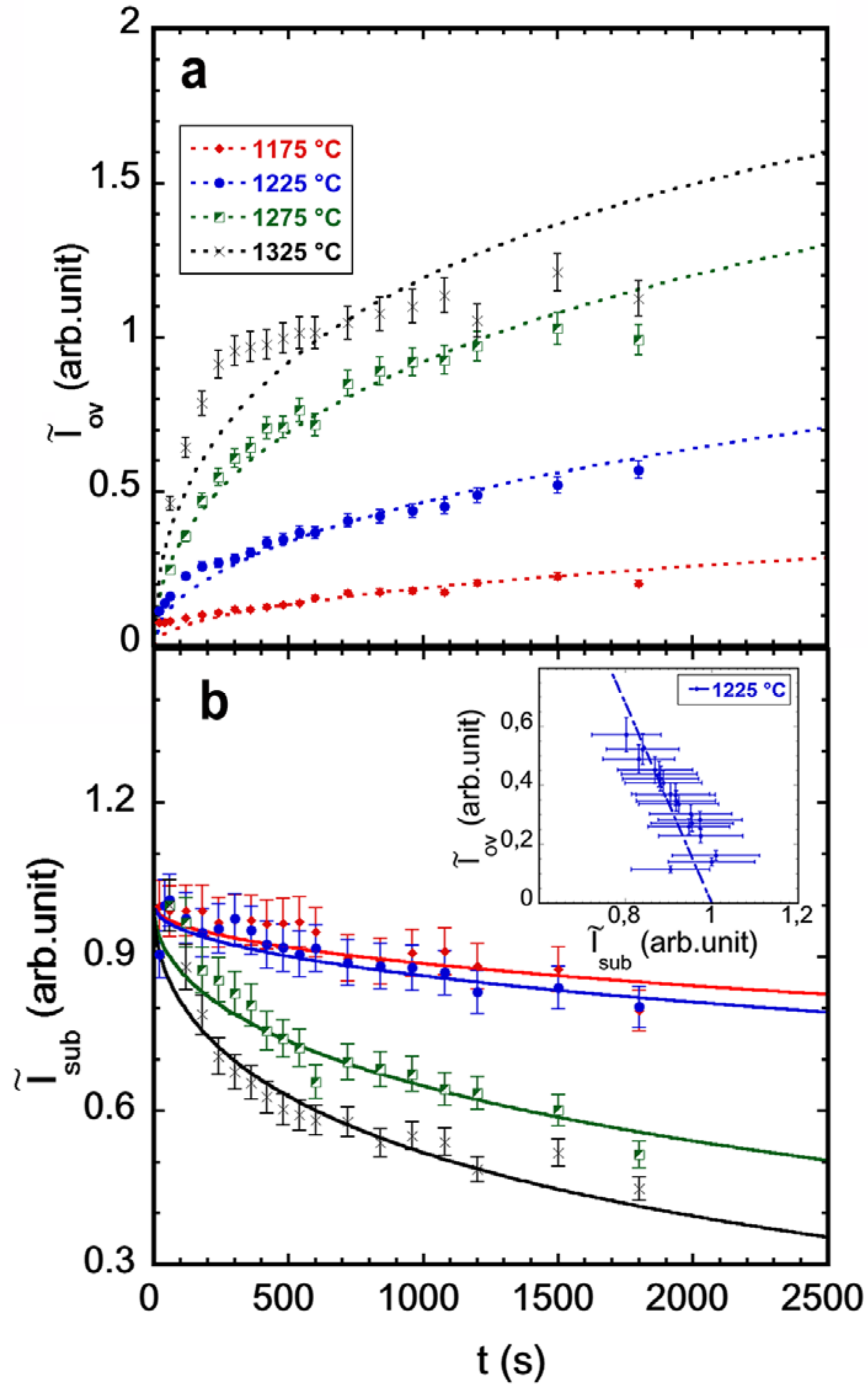

Figure 3: Time dependence of normalized C1s intensities from overlayer (a) and substrate (b). In panel (a) the best fit at each temperature with the exponential function in Eqn.2 is reported as dotted line. In panel (b) solid lines are the normalized intensities calculated through equation (3) using the fitting parameters as obtained from the fits of panel (a). An example of the linear behavior between $\tilde{I}_{ov}(t)$ and $\tilde{I}_{sub}(t)$ is displayed in the inset. The slope of the straight line provides the normalization factor m.

Here we notice that the validity of our approximation at all temperatures is confirmed also by the Arrhenius plot reported in Figure 4, where the values of *ln(β)* vs *1/T* are nicely aligned, providing an activation energy of 2.5±0.5 eV.

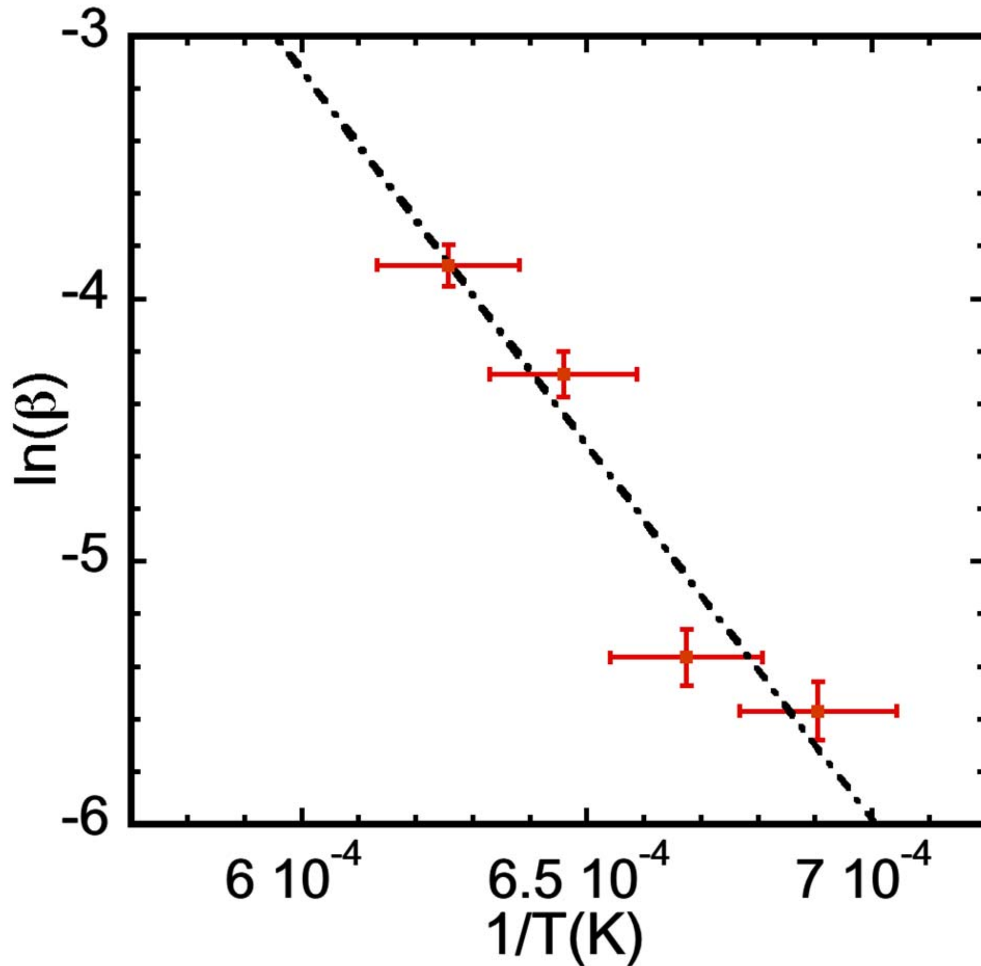

Figure 4: Arrhenius plot of the fitting parameter β: ln(β) vs 1/T

In order to understand the origin of the proposed power growth law, we need to analyze the experimental procedure employed to study the kinetics by means of successive steps of growth. We recall that each point on the curve of Figure 3 is linked to the growth of graphene on an already formed overlayer. We define $\Delta t=t_n-t_{n-1}$ as the elapsed time between two successive XPS measurements, where t_n is the time at step n. For the general growth law, $dh/dt=A/h^p$ [35, 36] (with A constant and $p \neq -1$), an integration between time t_{n-1} and t_n provides the thickness at running time t_n as a function of the thickness at time t_{n-1}:

$$h(t_n) = [A(p+1)(t_n - t_{n-1}) + h(t_{n-1})^{p+1}]^{1/(p+1)} \quad (6)$$

Iteration of Eqn.6 provides $h(t_n) = [A(p+1)(t_n) + h(0)^{p+1}]^{1/(p+1)}$ and as $h(0)=0$, we obtain the power law $h(t) = \lambda\beta t^{\gamma}$; $(\gamma = 1/(p+1))$. This argument gives support to our experimental procedure, based on repeated annealing and cooling of the sample, each followed by XPS measurement, matching our result ($\gamma=1/2$) for p=1.

4. Discussion

To have an insight into the growth law as obtained from the XPS data analysis, we developed a kinetic model, which takes into account the essential steps occurring during the epitaxial growth of graphene. To this end we refer to the bottom-up growth mechanism recently proposed in the literature, where graphene is continuously formed at the graphene-SiC interface during the Si evaporation [25] (Figure 2-I). The chemical processes leading to the growth of the overlayer can be schematized as follows:

$$SiC \rightarrow (Si)_v + C^* \quad (7)$$

$$C^* + G_n \rightarrow G_{n+1} \quad (8)$$

Reaction (7) describes the evaporation of Si, which produces "reactive" carbon species at the interface, here denoted as C^*, and Si in the gas phase (Si_v). While Si diffuses through the holes of the layers above, leaving the solid, (Figure 2) these reactive carbon units add to an already formed graphene layer (G_n) made up of n-C-units (Eqn. 8).

The present approach considers the reactions above to be rate determining, as far as the kinetics is concerned. Moreover the liberation of Si at the interface, for example through the formation of vacancies and interstitials, is assumed to occur under steady state conditions. Reaction (7) can be envisaged as a two step process as $SiC \leftrightarrow (Si)_i \rightarrow (Si)_v$ where $(Si)_i$ is an interstitial Si atom and the irreversible step implies diffusion of Si through the solid toward the vapor phase [24]. We can assume that the reaction for the formation of the interstitials proceeds under conditions not too far from equilibrium, leading to a time independent mole fraction of interstitials, as given by the law of mass action. At the kinetic level, this implies that for the reaction of interstitial formation the rate constant of the reverse reaction (vacancy-interstitial recombination) is larger than the inverse of the characteristic time of the diffusion process.

In the computation that follows we consider vertical diffusion of Si through the overlayer; the kinetics of this process is strictly dependent upon overlayer thickness. It is worth stressing that on the basis of phenomenological rate equations it is not possible to have an insight into the diffusion mechanism without independent information on diffusion barriers. Rate equations for the present modeling read:

$$\begin{cases} \frac{dn_{C^*}}{dt} = J_{Si} - K_2 n_{C^*} \\ \rho_G \frac{dh}{dt} = K_2 n_{C^*} \end{cases} \quad (9)$$

where n_{C^*} is the surface density of C^*, J_{Si} the flux of Si atoms which leave the interface, ρ_G the density of graphene, h the mean overlayer thickness and K_2 the (first order) rate constant of reaction (8), the attachment of C^* to the graphene network. The flux of Si atoms is modeled by means of Fick's first law as $J_{Si} = -D_{Si}\nabla c$ that is approximated according to $J_{Si} = D_{Si}\frac{c_i}{h} = \frac{K_1}{h}$, where D_{Si} and $c_i \equiv c_{(Si)_i}$ are the diffusion coefficient of Silicon in graphene through defects and concentration of mobile Si respectively. In particular, c_i is expected to depend exponentially on temperature, through the equilibrium constant of the reaction for interstitial Si formation $(Si)_i$. The reaction is $(Si)_{Si} + V_i \leftrightarrow (Si)_i + V_{Si}$, where V_i and V_{Si} denote interstitial and silicon vacancies, respectively and $(Si)_{Si}$ denotes a Si moving out from its lattice position. The equilibrium constant is equal to $K_e = c_{(Si)_i} c_{V_{Si}} = (c_i)^2$ that is further exploited to determine the rate constant K_1. Inserting the expression of J_{Si} in Eqn.9, the system of differential equations leads to:

$$\rho_G \frac{d^2h}{dt^2} = \frac{K_1 K_2}{h} - \rho_G K_2 \frac{dh}{dt} \quad (10)$$

Let us define the dimensionless variables $\tau = K_2 t$ and $\bar{h} = h/h_o$, being h_o the initial thickness of the overlayer, and the function $z(\tau) = \left(\frac{d\bar{h}}{d\tau}\right)^2$ In terms of these variables Eqn.(10) reduces to the following first order differential equation,

$$\frac{1}{2}\frac{dz}{d\bar{h}} + \sqrt{z} = \frac{B}{\bar{h}} \quad (11)$$

where $B = \frac{K_1}{K_2}\frac{1}{\varrho_G h_o^2}$. The constant B depends on temperature through the K_i rate constants. In fact $K_1 \approx \exp\left[-\frac{U_d^* + \frac{E_{Si}}{2}}{k_B T}\right]$ and $K_2 \approx \exp\left[-\frac{U_C^*}{k_B T}\right]$, where U_d^* is the activation energy for Si diffusion in the overlayer and E_{Si} the energy (standard enthalpy change) for the formation of interstitials i.e. for the

liberation of Si atoms while U_C^* is the effective activation energy for the reaction (8), provided the reaction for the attachment of *C* units is energy activated.

From the knowledge of the solution of Eqn.11 the growth law *h=h(t)* can be eventually determined through inversion of the $\tau \equiv \tau(\bar{h})$ function given by

$$\tau(\bar{h}) = \int_1^{\bar{h}} \frac{d\bar{h}}{\sqrt{z(\bar{h})}}. \tag{12}$$

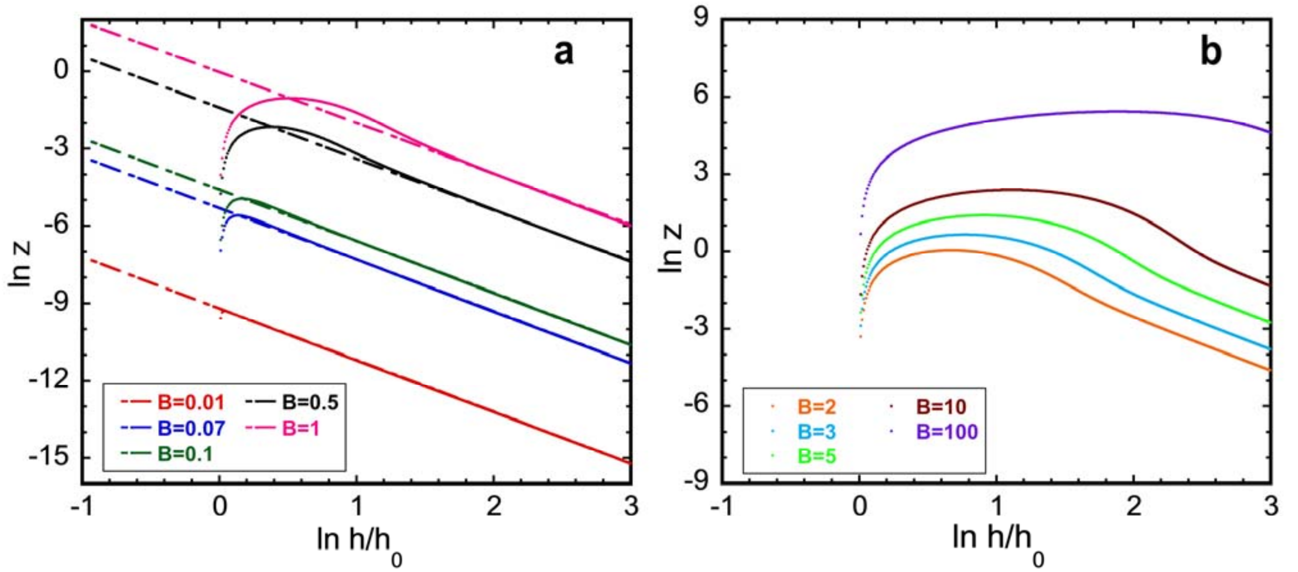

Figure 5: a) Numerical solutions of differential equation (11) for B≤1. The straight lines imply a power growth law with exponent γ=1/2. (b) The numerical solutions of Eqn.11 for B>1 exhibit a non linear behavior of ln(z) vs ln(h/h$_o$*)*.

Eqn. 11 has been solved, numerically, as a function of the *B* parameter with initial condition *z(1)=0*. Typical solutions $z(\bar{h}; B)$ are reported in Figure 5 on double logarithmic scale. The behavior of z is found to depend strongly on *B,* namely on whether *B* is higher or lower than unity. The value *B=1* defines the transition between two growth regimes. For *B<1* the kinetics is in agreement with the equation $\ln(z) = B - 2\ln(\bar{h})$ (Figure 5a) which implies $\frac{d\bar{h}}{d\tau} = \frac{B}{\bar{h}}$ and leads to the growth law:

$$h(t) = \left(\frac{2K_1}{\varrho_G}\right)^{1/2} t^{1/2} \tag{13}$$

with exponent equal to 1/2. On the other hand, for *B>1* the kinetics exhibits a complex behavior which can be characterized, in a phenomenological way, by means of a time dependent growth exponent. The kinetic law (Eqn.13) does show that an Arrhenius plot of the multiplicative constant $(\lambda\beta) = \left(\frac{2K_1}{\varrho_G}\right)^{1/2}$

(Figure 4) gives an "apparent" activation energy $E_a = \frac{U_d^* + \frac{E_{Si}}{2}}{2}$, which depends upon both kinetic and thermodynamic quantities. In the growth regime where $B<1$, the evaporation of Silicon (Eqn. 7) is rate determining, whereas for $B > 1$ the transformation of C in graphene (Eqn. 6) is rate determining.

There is also an intermediate range of growth, around $B \approx 1$ where both processes proceed at a comparable rate. On the basis of the XPS data analysis, which results in the exponent $\gamma = 1/2$, the proposed approach lends support to a growth mechanism where the diffusion of Si through graphene is rate determining. In fact when $K_1 << K_2$ we have $B<1$ (Eqn. 11). This condition is well verified for the first three temperatures (1175<T<1275 ˚C) (see Figure 3), as witnessed by the good fit of Eqn. (13) to the experimental data. At T =1325 ˚C the fit worsen, suggesting that the condition $B<1$ is not well satisfied in this case. At this temperature the growth law is expected to und undergo a transition from $B<1$ to $B \approx 1$, while the condition $B>1$ is expected to hold at higher temperatures [37]. This is in agreement with the suggestion that the diffusion of Si through the step edge becomes a facile route for Si evaporation, which happens as soon as the top layer is completed. However, the diffusion through defects still holds for the layers below.

By analyzing the results of the Arrhenius plot of the β coefficient, as obtained by fitting the experimental kinetics (Figure 4) we observe that the apparent activation energy, E_a = 2.5±0.5 eV, matches our previous result [38], and we relate this Figure to the "effective" activation energy for graphene growth, entering the rate constant K_1, for which we obtain the value $U_d^* + \frac{E_{Si}}{2}$ that is equal to $2E_a = 5 \pm 1$ eV. First principles calculations of the energy barrier for vertical diffusion of Si in the $6\sqrt{3} \times 6\sqrt{3}$ interface layer gives a value of 4.7 eV, corresponding to U_d^*, and a value of 3.2 eV to break the bond of a Si atom in SiC (corresponding to E_{Si}) [2], providing a theoretical estimation of the effective barrier for graphene formation $U_d^* + \frac{E_{Si}}{2} \approx 6 \pm 1$ eV. We notice that this value matches, within the experimental error, our results. The small difference could be assigned to variations of the energy barrier due to the presence of defects at the interface or to the fact that under growth conditions (bottom-up growth) the composition of the substrate surface changes in time affecting the mean value of the energy for Si liberation.

In addition, we remark that with reference to the process of Si evaporation our experiment is performed under conditions far from equilibrium: the vapor pressure of Si in the chamber is several order of magnitudes lower than the equilibrium value [39, 40]. Under these circumstances it is compulsory to

focus on the kinetics of the reaction, and the simplest way to accomplish this task is to employ phenomenological rate equations as discussed in this work. Regarding the assumptions that validate the kinetic approach, we note that Eqn.10 has been obtained on the basis of the steady state approximation, which is consistent with quasi-equilibrium conditions for the reaction of interstitial formation at the interface. In fact, it is possible to show that quasi-equilibrium implies $e^{-E_{Si}/2KT} \gg e^{-U_d^*/KT}$ which is shown to hold for the system here investigated. Before concluding, we briefly discuss the present results in connection with a model recently developed in the literature for graphene growth by evaporation. It was shown in ref [41, 42] that on the C-face of 6H-SiC(000$\bar{1}$) graphene formation may occur through nucleation and lateral growth of graphene nuclei with constant thickness. It is worth stressing that this study refers to temperature deposition well above the temperature range here investigated and under high Ar pressure. Also, the SiC surface is different from the one here studied. We note that a lateral growth mechanism does not fully explain our XPS data. In fact, as regards the behavior of both $I_{ov}(t)$ and $I_{sub}(t)$ intensity, such a growth mode would imply: $\frac{I_{ov}(t)}{I_{ov}^{\infty}} = S(t)\left(1 - e^{-h/\lambda}\right)$ and $\frac{I_{sub}(t)}{I_{sub}^{0}} = \left[1 - S(t)\left(1 - e^{-h/\lambda}\right)\right]$ where $S(t)$ is the surface fraction covered by graphene and h the constant value of the thickness of graphene nuclei. By applying this model to our data we find that the behavior of the substrate intensity is satisfactorily described by the equation above for $S(t) \approx t^k$ (with $k \approx 0.5$); however, this $S(t)$ function does not match our experimental data of the overlayer intensity, which can be fitted only by a stretched exponential curve (Eqn. 2). Moreover, $S(t) \approx t^{1/2}$ would imply a lateral growth law $l(t) \approx t^{1/4}$ which is not consistent with a diffusion mediated growth mode.

The present discussion put in evidence the complexity of the mechanism which rules the graphene growth which is found to be strongly dependent on the substrate surface (Si-face or C-face), surface temperature, impurity in the gas phase and pressure.

5. Conclusions

In conclusion, on the basis of XPS data, we derived a model for graphene growth on 3C SiC (111)/Si (111) by Si sublimation as a function of time and of annealing temperature, suggesting a bottom-up growth governed by a square root law. Our model indicates that Si diffusion across graphene overlayer,

occurring under conditions far from equilibrium, is the rate limiting step of the growth up to 1275°C. The kinetic approach deals with an interface characterized by a high defect density, needed for a high Si mobility. At higher temperatures, when the overlayer is completed, the diffusion to the step edges becomes the only facile route for Si evaporation, slowing down considerably the growth. An effective activation energy for graphene growth (~5eV) has been estimated, in good agreement with the theoretical value obtained from first principles calculations. Such an agreement lends support to the present kinetic-thermodynamic model, which can be profitably exploited to describe other systems.

Acknowledgements

The authors acknowledge the support of the Australian Research Council (ARC) through the Discovery project DP130102120, the Marie Curie International Research staff Exchange Scheme Fellowship within the 7th European Community Framework Programme, and the Australian National Fabrication Facility. FI is recipient of a Future Fellowship from the Australian Research Council (FT120100445). The technical support of Dr. Peter Hines at the Central Analytical Research Facility of the Institute of Future Environments as well as the funding by the ARC through the LIEF grant (LE100100146) are also kindly acknowledged. The authors would like to thank Dr Jennifer MacLeod for critical reading of the manuscript.

References

[1] Murali, R., *Graphene Nanoelectronics: From Materials to Circuits*2012: Springer-Verlag New York. 265.

[2] Varghese, S.S., S. Lonkar, K.K. Singh, S. Swaminathan, and A. Abdala, *Recent advances in graphene based gas sensors.* Sensors and Actuators B: Chemical, 2015. **218**(0): p. 160-183.

[3] Galpaya, D., M. Wang, M. Liu, N. Motta, E.R. Waclawik, and C. Yan, *Recent advances in fabrication and characterization of graphene-polymer nanocomposites.* Graphene, 2012. **1**(2): p. 30-49.

[4] Bonaccorso, F., L. Colombo, G. Yu, M. Stoller, V. Tozzini, A.C. Ferrari, R.S. Ruoff, and V. Pellegrini, *Graphene, related two-dimensional crystals, and hybrid systems for energy conversion and storage.* Science, 2015. **347**(6217).

[5] Emtsev, K.V., A. Bostwick, K. Horn, J. Jobst, G.L. Kellogg, L. Ley, J.L. McChesney, T. Ohta, S.A. Reshanov, J. Rohrl, E. Rotenberg, A.K. Schmid, D. Waldmann, H.B. Weber, and T. Seyller, *Towards wafer-size graphene layers by atmospheric pressure graphitization of silicon carbide.* Nat Mater, 2009. **8**(3): p. 203-207.

[6] de Heer, W.A., C. Berger, M. Ruan, M. Sprinkle, X. Li, Y. Hu, B. Zhang, J. Hankinson, and E.H. Conrad, *Large area and structured epitaxial graphene produced by confinement controlled sublimation of silicon carbide.* Proceedings of the National Academy of Sciences, 2011. **108**(41): p. 16901.

[7] Ouerghi, A., M.G. Silly, M. Marangolo, C. Mathieu, M. Eddrief, M. Picher, F. Sirotti, S. El Moussaoui, and R. Belkhou, *Large-Area and High-Quality Epitaxial Graphene on Off-Axis SiC Wafers.* Acs Nano, 2012. **6**(7): p. 6075-6082.

[8] Tromp, R.M. and J.B. Hannon, *Thermodynamics and Kinetics of Graphene Growth on SiC(0001).* Physical Review Letters, 2009. **102**(10): p. 106104.

[9] Badami, D.V., *Graphitization of [alpha]-Silicon Carbide.* Nature, 1962. **193**(4815): p. 569-570.

[10] Emtsev, K.V., F. Speck, T. Seyller, L. Ley, and J.D. Riley, *Interaction, growth, and ordering of epitaxial graphene on SiC {0001} surfaces: A comparative photoelectron spectroscopy study.* Physical Review B, 2008. **77**(15): p. 155303.

[11] Goler, S., C. Coletti, V. Piazza, P. Pingue, F. Colangelo, V. Pellegrini, K.V. Emtsev, S. Forti, U. Starke, and F. Beltram, *Revealing the atomic structure of the buffer layer between SiC (0001) and epitaxial graphene.* Carbon, 2013. **51**: p. 249-254.

[12] Ouerghi, A., A. Kahouli, D. Lucot, M. Portail, L. Travers, J. Gierak, J. Penuelas, P. Jegou, A. Shukla, and T. Chassagne, *Epitaxial graphene on cubic SiC (111)/Si (111) substrate.* Applied Physics Letters, 2010. **96**(19): p. 191910-191910-3.

[13] Riedl, C., C. Coletti, and U. Starke, *Structural and electronic properties of epitaxial graphene on SiC (0 0 0 1): a review of growth, characterization, transfer doping and hydrogen intercalation.* Journal of Physics D: Applied Physics, 2010. **43**: p. 374009.

[14] Riedl, C., U. Starke, J. Bernhardt, M. Franke, and K. Heinz, *Structural properties of the graphene-SiC (0001) interface as a key for the preparation of homogeneous large-terrace graphene surfaces.* Physical Review B, 2007. **76**(24): p. 245406.

[15] Sforzini, J., L. Nemec, T. Denig, B. Stadtmüller, T.L. Lee, C. Kumpf, S. Soubatch, U. Starke, P. Rinke, V. Blum, F.C. Bocquet, and F.S. Tautz, *Approaching Truly Freestanding Graphene: The Structure of Hydrogen-Intercalated Graphene on 6H-SiC(0001).* Physical Review Letters, 2015. **114**(10): p. 106804.

[16] Riedl, C., C. Coletti, T. Iwasaki, A.A. Zakharov, and U. Starke, *Quasi-Free-Standing Epitaxial Graphene on SiC Obtained by Hydrogen Intercalation.* Physical Review Letters, 2009. **103**(24): p. 246804.

[17] Nemec, L., V. Blum, P. Rinke, and M. Scheffler, *Thermodynamic Equilibrium Conditions of Graphene Films on SiC.* Physical Review Letters, 2013. **111**(6): p. 065502.

[18] Qi, Y., S.H. Rhim, G.F. Sun, M. Weinert, and L. Li, *Epitaxial Graphene on SiC(0001): More than Just Honeycombs.* Physical Review Letters, 2010. **105**(8): p. 085502.

[19] Emery, J.D., B. Detlefs, H.J. Karmel, L.O. Nyakiti, D.K. Gaskill, M.C. Hersam, J. Zegenhagen, and M.J. Bedzyk, *Chemically Resolved Interface Structure of Epitaxial Graphene on SiC(0001).* Physical Review Letters, 2013. **111**(21): p. 215501.

[20] Hass, J., F. Varchon, J.E. Millán-Otoya, M. Sprinkle, N. Sharma, W.A. de Heer, C. Berger, P.N. First, L. Magaud, and E.H. Conrad, *Why Multilayer Graphene on 4HSiC(0001) Behaves Like a Single Sheet of Graphene.* Physical Review Letters, 2008. **100**(12): p. 125504.

[21] Mallet, P., F. Varchon, C. Naud, L. Magaud, C. Berger, and J.Y. Veuillen, *Electron states of mono- and bilayer graphene on SiC probed by scanning-tunneling microscopy.* Physical Review B, 2007. **76**(4): p. 041403.

[22] Wang, D., L. Liu, W. Chen, X. Chen, H. Huang, J. He, Y.-P. Feng, A.T.S. Wee, and D.Z. Shen, *Optimized growth of graphene on SiC: from the dynamic flip mechanism.* Nanoscale, 2015. **7**(10): p. 4522-4528.

[23] Yazdi, G.R., R. Vasiliauskas, T. Iakimov, A. Zakharov, M. Syväjärvi, and R. Yakimova, *Growth of large area monolayer graphene on 3C-SiC and a comparison with other SiC polytypes.* Carbon, 2013. **57**: p. 477-484.

[24] Sun, G.F., Y. Liu, S.H. Rhim, J.F. Jia, Q.K. Xue, M. Weinert, and L. Li, *Si diffusion path for pit-free graphene growth on SiC (0001).* Physical Review B, 2011. **84**(19): p. 195455.
[25] Huang, H., W. Chen, S. Chen, and A.T.S. Wee, *Bottom-up growth of epitaxial graphene on 6H-SiC (0001).* Acs Nano, 2008. **2**(12): p. 2513-2518.
[26] Hannon, J.B., M. Copel, and R.M. Tromp, *Direct Measurement of the Growth Mode of Graphene on SiC(0001) and SiC(000-1).* Physical Review Letters, 2011. **107**(16): p. 166101.
[27] Tanaka, S., K. Morita, and H. Hibino, *Anisotropic layer-by-layer growth of graphene on vicinal SiC (0001) surfaces.* Physical Review B, 2010. **81**(4): p. 041406.
[28] Drabińska, A., K. Grodecki, W. Strupiński, R. Bożek, K.P. Korona, A. Wysmołek, R. Stępniewski, and J.M. Baranowski, *Growth kinetics of epitaxial graphene on SiC substrates.* Physical Review B, 2010. **81**(24): p. 245410.
[29] Wang, L., S. Dimitrijev, J. Han, A. Iacopi, L. Hold, P. Tanner, and H.B. Harrison, *Growth of 3C–SiC on 150-mm Si (100) substrates by alternating supply epitaxy at 1000° C.* Thin solid films, 2011. **519**(19): p. 6443-6446.
[30] Gupta, B., E. Placidi, C. Hogan, N. Mishra, F. Iacopi, and N. Motta, *The transition from 3C SiC(111) to graphene captured by Ultra High Vacuum Scanning Tunneling Microscopy.* Carbon, 2015. **91**(0): p. 378-385.
[31] Sutter, P., *Epitaxial graphene: How silicon leaves the scene.* Nat Mater, 2009. **8**(3): p. 171-172.
[32] Starke, U., C. Coletti, K. Emtsev, A.A. Zakharov, T. Ouisse, and D. Chaussende. *Large Area Quasi-Free Standing Monolayer Graphene on 3C-SiC (111)*. in *Materials Science Forum*. 2012. Trans Tech Publ.
[33] Tougaard, S. *QUASES-IMFP-TPP2M program*. http://www.quases.com/products/quases-tougaard/, accessed 1 August 2015.
[34] Gupta, B., M. Notarianni, N. Mishra, M. Shafiei, F. Iacopi, and N. Motta, *Evolution of epitaxial graphene layers on 3C SiC/Si (111) as a function of annealing temperature in UHV.* Carbon, 2014. **68**: p. 563-572.
[35] Lawless, K.R., *The oxidation of metals.* Reports on Progress in Physics, 1974. **37**(2): p. 231.
[36] Tomasini, P., V. Machkaoutsan, and S.G. Thomas, *A power rate law study of silicon germanium selective vapor phase epitaxy kinetics.* Materials Science in Semiconductor Processing, 2009. **12**(3): p. 126-131.
[37] Drabińska, A., K. Grodecki, W. Strupiński, R. Bożek, K. Korona, A. Wysmołek, R. Stępniewski, and J. Baranowski, *Growth kinetics of epitaxial graphene on SiC substrates.* Physical Review B, 2010. **81**(24): p. 245410.
[38] Gupta, B., M. Notarianni, N. Mishra, M. Shafiei, F. Iacopi, and N. Motta, *Corrigendum to "Evolution of epitaxial graphene layers on 3C SiC/Si (111) as a function of annealing temperature in UHV" [Carbon 68 (2014) 563–572].* Carbon, 2015. **84**: p. 280.
[39] Tromp, R. and J. Hannon, *Thermodynamics and kinetics of graphene growth on SiC (0001).* Physical Review Letters, 2009. **102**(10): p. 106104.
[40] Lilov, S.K., *Thermodynamic analysis of phase transformations at the dissociative evaporation of silicon carbide polytypes.* Diamond and Related Materials, 1995. **4**(12): p. 1331-1334.
[41] Norimatsu, W., J. Takada, and M. Kusunoki, *Formation mechanism of graphene layers on SiC (000$\overline{1}$) in a high-pressure argon atmosphere.* Physical Review B, 2011. **84**(3): p. 035424.
[42] Wataru, N. and K. Michiko, *Growth of graphene from SiC{0001} surfaces and its mechanisms.* Semiconductor Science and Technology, 2014. **29**(6): p. 064009.